Biogeosciences
Discussions

Open Access

Validation of the Thorpe scale-derived vertical diffusivities against microstructure measurements in the Kerguelen region

Y.-H. Park[1], J.-H. Lee[2], I. Durand[1], and C.-S. Hong[2]

[1]MNHN-Sorbonne Universités (UPMC, Univ Paris 06)-CNRS-IRD, LOCEAN Laboratory, Muséum National d'Histoire Naturelle, 43, rue Cuvier, 75005 Paris, France
[2]Korea Institut of Ocean Science & Technology, Ansan, Korea

Correspondence to: Y.-H. Park (yhpark@mnhn.fr)

Discussion Paper | Discussion Paper | Discussion Paper | Discussion Paper |

BGD
11, 12137–12157, 2014

Validation of the Thorpe scale-derived vertical diffusivities

Y.-H. Park et al.

Title Page

Abstract | Introduction
Conclusions | References
Tables | Figures

◀ | ▶
◀ | ▶

Back | Close

Full Screen / Esc

Printer-friendly Version

Interactive Discussion

Abstract

The Thorpe scale is an energy containing vertical overturning scale of large eddies associated with shear generated turbulence. We make here indirect estimates of vertical diffusivities from the Thorpe scale method in the Polar Front region east of the Kerguelen Islands based on fine scale density profiles gathered during the 2011 KEOPS2 cruise. These are validated in comparison with diffusivities estimated from the turbulence dissipation rate directly measured via a TurboMAP microprofiler. The results are sensitive to the choice of the diffusivity parameterization and the Gargett and Garner's (2008) overturn ratio R_o, with the optimal results showing an agreement within a factor of 4, on average, having been obtained from the parameterization by Shih et al. (2005) and the $R_o = 0.25$ criterion.

The Thorpe scale-derived diffusivities in the KEOPS2 region show a high degree of spatial variability, ranging from a canonical value of O($10^{-5}\,\mathrm{m^2\,s^{-1}}$) in the Winter Water layer and in the Subantarctic surface waters immediately north of the Polar Front to a high value of O($10^{-4}\,\mathrm{m^2\,s^{-1}}$) in the seasonal thermocline just below the surface mixed layer. The latter values are found especially over the shallow plateau southeast of the Kerguelen Islands and in the Antarctic surface waters associated with the Polar Front attached to the escarpment northeast of the islands.

1 Introduction

Vertical mixing is a dominant factor in controlling vertical fluxes of heat, salt, and nutrients, so the estimation of vertical (or diapycnal) diffusivities especially in the upper layer of the ocean was one of the primary priorities of the physical component of the KEOPS2 cruise. During the cruise, direct turbulence measurements were made at selected stations using a tethered quasi-freefall profiler, TurboMAP, measuring the microstructure of velocity shear. An indirect method for estimating vertical diffusivities using more accessible CTD (Conductivity-Temperature-Depth) density profiles is the Thorpe scale

Validation of the Thorpe scale-derived vertical diffusivities

Y.-H. Park et al.

method (Thorpe, 1977). The objective of this study is to estimate the vertical diffusivities from fine scale density profiles using the Thorpe scale method and validate them in comparison with microstructure measurements collected via a TurboMAP during the KEOPS2 cruise.

The performance of the Thorpe scale method compared to microstructure estimates has been known to depend on the stratification of the water column and surface environment conditions affecting the ship motion. While good agreement between the two methods has been reported in low-latitude regions of high stratification and low winds (Ferron et al., 1998; Klymak et al., 2008), the application of the Thorpe scale method in the Southern Ocean can be compromised because of low stratification and extreme environments (Frants et al., 2013). The latter authors reported that the CTD-based fine structure methods overestimate microstructure diffusivities by one to two orders of magnitude in the southeastern Pacific and Drake Passage, claiming their real limitations in the Southern Ocean.

Another intriguing issue concerns the existence of two different parameterizations of vertical diffusivity K in terms of turbulence dissipation rate ε and buoyancy frequency N. Note that $N^2 = -(g/\rho_0)\rho_z$, where g is gravity, ρ_0 is a constant reference density, and ρ_z is a vertical gradient of potential density calculated at each depth over a vertical extent of 10 m.

For example, Osborn (1980) suggested a well-known parameterization as

$$K = 0.2\varepsilon/N^2. \tag{1}$$

On the other hand, Shih et al. (2005) recently proposed, based on the laboratory and numerical experiments, a new parameterization for the energetic turbulence regime ($\varepsilon/\nu N^2 > 100$) as

$$K = 2\nu(\varepsilon/\nu N^2)^{1/2}, \tag{2}$$

where $\nu = (1.5\text{–}1.8)\,10^{-6}\,\mathrm{m^2\,s^{-1}}$ is the kinematic viscosity in the temperature range of 0–5 °C and $\varepsilon/\nu N^2$ is the turbulence intensity parameter. Note that for the moder-

ate turbulence intensity regime ($7 < \varepsilon/\nu N^2 < 100$), the parameterization of K by Shih et al. (2005) is same as Eq. (1) proposed by Osborn (1980).

While the TurboMAP measurements lead to direct estimates of ε, the Thorpe scale method gives its indirect estimates by making use of an empirical relationship between the Thorpe scale and ε. These two (direct and indirect) estimates of ε can be applied to the above two parameterizations of K, yielding a total of four kinds of estimates at each station of intercomparison. Because of their utmost importance, the detailed procedures for the preliminary processing of CTD data as well as for the detection and validation of overturns for calculating the Thorpe scale are given in Sect. 2. These are largely based on a comprehensive paper by Gargett and Garner (2008), although we have added some modifications. We will show in Sect. 3 that the results are sensitive to the choice of the K parameterization and to the criteria of the overturn validation. In Sect. 4 we present vertical diffusivities in the KEOPS2 area estimated from the optimally chosen parameterization and overturn ratio. The concluding remarks are given in Sect. 5.

2   Preliminary processing of CTD data

CTD data used for deriving fine scale density profiles were collected during the October–November 2011 KEOPS2 cruise aboard the R/V *Marion Dufresne* in the Polar Front region east of the Kerguelen Islands (Park et al., 2014, for details of the regional hydrography and frontal circulation). We used here a total of 22 CTD profiles gathered using two sets of Sea-Bird SBE 9*plus* sensors at stations shown in Fig. 1, where the concomitant TurboMAP stations are shown circled. The CTD profiles mostly extend from the surface to the bottom, while the TurboMAP measurements to about 400 m from the surface, limiting our validation of the Thorpe scale method to the top 400 m.

A critical step to a successful validation of the latter method resides in the minimization of the effects of instrument noise and measurement errors, which may be due to the conductivity cell's thermal lag, pressure reversals due to ship roll, and salinity spik-

ing caused by the differing time responses of the temperature and conductivity sensors (e.g. Gargett and Garner, 2008). A series of procedures for processing CTD data are given below.

1. For minimizing thermal lag arising from the conductivity cell thermal mass effects, the raw CTD data have been first processed using the Sea-Bird processing software (http://www.seabird.com/pdf_documents/manuals/SBEDataProcessing_7.23.2.pdf). The data processing module "Cell Thermal Mass" performs conductivity thermal mass correction, for which we used typical values ($\alpha = 0.03; 1/\beta = 7.0$) recommended for SBE 9*plus*.

2. Salinity spiking, which can be caused by misalignment of temperature and conductivity with each other, was removed on acquisition from a pre-programmed SBE 9*plus* deck unit by advancing conductivity by 0.073 s. Therefore, there is no need to run the data processing module "Align CTD".

3. Due to the effect of the ship heave motion on the hard-coupled CTD, the fall speed of CTD continuously varies while scanning and can occasionally reverse sign for short periods. We located segments of pressure reversals and edited out the data between successive encounters of the same pressure, although such can be also done via the data processing module "Loop Edit".

4. At this stage, the CTD conductivity and salinity data were corrected with water bottle salinity previously analyzed using a salinometer.

5. In order to further minimize any spike-like anomalies in property (salinity, potential temperature, potential density) profiles, we applied a quadratic fit to successive 10 m segments to detect and discard "extremely abnormal" anomalies surpassing 4 times the root mean square (rms) anomaly relative to the fitting curve. About 0.03 % of total scans are eliminated by this process.

6. Our final CTD data processing consisted of averaging and subsampling profiles at regular depth intervals. For this, we averaged the property profiles over a 10 cm

Full Screen / Esc

Printer-friendly Version

Interactive Discussion

Full Screen / Esc

Printer-friendly Version

Interactive Discussion

window that is centered at each depth incremented by a regular span of 10 cm. On average, about 2–3 scans enter into this 10 cm averaging, which is roughly consistent with a mean fall rate of $\sim 0.9 \, \text{m s}^{-1}$ of our 24 Hz CTD. This filters out any high-frequency random noise of a length scale less than 10 cm, thus the smallest detectable overturn should be of 20 cm in vertical extent. Note also that most density profiles start from 20 m below the sea surface because the near-surface measurements are often found to be much contaminated probably by turbulence generated by the hull. These processed density profiles form our basic data set used in the following section.

3 Thorpe scale analysis

3.1 Thorpe scale and vertical diffusivity

A first step for detecting overturns generated by turbulence in a stratified water column consists of sorting a potential density profile $\rho(z)$, which may contain inversions, into a stable monotonic sequence without inversions. The vertical displacement necessary for generating the stable profile is the Thorpe displacement ζ, and the Thorpe scale L_{T} is defined as the rms of ζ within each overturn that is a region over which the sum of ζ drops back to zero (Dillon, 1982).

On the other hand, a classical measure of the overturning length is the Ozmidov scale L_{O} (Ozmidov, 1965) defined as

$$\varepsilon = L_{\text{O}}^2 N^3. \tag{3}$$

Dillon (1982) suggested a linear relationship between L_{T} and L_{O}, such as

$$L_{\text{O}} = 0.8(\pm 0.4) L_{\text{T}}, \tag{4}$$

although an exact linear relation between these two overturning scales cannot be expected due to spatial and temporal variability of the turbulent field (Ferron et al., 1998).

Inserting Eqs. (3) and (4) into Eqs. (1) and (2), the vertical diffusivity can be estimated indirectly from L_T as

$$K = 0.128L_T^2N, \tag{5}$$

according to the Osborn parameterization, and as

$$K = 1.6\nu^{1/2}L_TN^{1/2}, \tag{6}$$

according to the Shih parameterization. We give below a series of procedures necessary for an optimal estimation of L_T, thus of K from the Thorpe scale method.

3.2 Determination of a threshold noise level of density

The major concern in the overturn validation is whether the identified overturns are false overturns associated with random noise and/or residual effects of salinity spiking. To prevent false overturns due to random noise, we followed an intermediate density profile method proposed by Gargett and Garner (2008) who modified a profile processing method of Ferron et al. (1998). The Gargett and Garner's method tracks only significant differences in the density profile, where a significant difference is defined relative to a threshold noise level below which a density difference is considered as due to random noise. For this purpose, we have calculated the rms of detrended density anomalies over successive 10 m segments for selected "well-mixed" layers within the cruise data set. This yielded a mean value of $1.75 \times 10^{-4}\,\mathrm{kg\,m^{-3}}$. We considered a multiple of 4 of the latter value, $7 \times 10^{-4}\,\mathrm{kg\,m^{-3}}$, as our threshold noise level. Note that the latter value is close to $5 \times 10^{-4}\,\mathrm{kg\,m^{-3}}$ of Gargett and Garner (2008) who applied instead a multiple of 5 to a slightly smaller mean rms density anomaly of $1.0 \times 10^{-4}\,\mathrm{kg\,m^{-3}}$ obtained in the Ross Sea region using a similar SBE 9*plus* CTD.

3.3 Creation of an intermediate density profile

Once the threshold value is determined as above, building an intermediate density profile is straightforward as clearly explained in Gargett and Garner (2008). Shortly

Full Screen / Esc

Printer-friendly Version

Interactive Discussion

speaking, an intermediate profile is created first from the top to the bottom, maintaining a constant density until a density change greater than the threshold value. A similar profile starting from the bottom to the top is also created and a finale intermediate profile used here is the average of the two individual (downward and upward) profiles.

5   An example of this procedure for determining an intermediate density profile is shown in Fig. 2.

3.4   Validation of overturns

Gargett and Garner (2008) reviewed several previous methods of overturn validation and proposed a practical method using an overturn ratio, $R_o = \min(L^+/L, L^-/L)$, where
10   L is the total vertical extent of an overturn and L^+ (L^-) is the cumulative extent occupied by positive (negative) Thorpe displacements ζ. These authors found the T–S tightness method suggested by Galbraith and Kelly (1996) unsatisfactory and did not recommend any further rejection based on any measure of T–S tightness. Gargett and Garner (2008) reasoned that a single perfect overturn sampled straight through the middle
15   would contain equal lengths of positive and negative ζ (or $R_o = 0.5$), and suggested a critical R_o value of 0.2, below which the prospect overturn is suspected of being caused by residual salinity spiking.

We found that this criterion ($R_o = 0.2$) is not sufficient in our case, but the use of $R_o = 0.25$ at least is rather necessary to detect the false overturns associated with
20   suspicious salinity spiking. An example is given in Fig. 3 for station A3-1, where we observe four most apparent density spikes as indicated by arrows. The first two spikes near 200 and 225 m pass marginally the ($R_o =$) 0.25 criterion but not the 0.2 criterion. The third spike just above 300 m passes without difficulty even the 0.2 criterion, while for the spike just below 300 m, the 0.25 criterion appears to be absolutely necessary.
25   In summary, all four suspected false overturns can be safely detected only by our new criterion, $R_o = 0.25$. We will show below that these four suspicious overturns really correspond to false overturns.

3.5 Sensitivity of the vertical diffusivity to its parameterization

With the Thorpe scales L_T obtained based on the $R_o = 0.25$ criterion, we have calculated vertical diffusivities from the Osborn and Shih parameterizations (Eqs. 5 and 6), denoted hereafter as K_{O_T} and K_{S_T}, respectively. The regions where no overturns are detected do not necessarily mean no vertical mixing, as already remarked by Ferron et al. (1998), but our method cannot resolve tiny overturns smaller than 20 cm, as mentioned in Sect. 2. In this case the corresponding diffusivities are set to $10^{-5}\,\mathrm{m^2\,s^{-1}}$, a value close to the minimum of the TurboMAP-derived diffusivities in our study area. The resulting diffusivities have been averaged over regular vertical intervals of 10 m. These Thorpe scale-derived diffusivities at station A3-1, as an example, are compared in Fig. 4 with those calculated according to Eqs. (1) and (2) using the TurboMAP-derived ε, denoted hereafter as K_{O_E} and K_{S_E}, respectively (Fig. 4c). We also show in the same figure K_{O_T} and K_{S_T} estimated using the $R_o = 0.2$ criterion, always in comparison with K_{O_E} and K_{S_E} (Fig. 4b). Several interesting features appear. First, the Thorpe scale-derived diffusivities for the case of $R_o = 0.2$ are systematically overestimated compared to the TurboMAP-derived diffusivities by up to one to two orders of magnitude in the layer below 80 m, while the converse is true above it in the surface mixed layer. Second, such an overestimation or underestimation in the Thorpe scale-derived diffusivities is much more pronounced by an order of magnitude with the Osborn parameterization (K_{O_T}) compared to the Shih parameterization (K_{S_T}). Third, the TurboMAP-derived diffusivities from both parameterizations (K_{O_E} and K_{S_E}) agree with each other within a factor of 2, on average, except for the surface mixed layer where the difference reaches up to an order of magnitude. As compared to K_{S_E}, there appears a tendency of great overestimation (slight underestimation) of K_{O_E} in the surface mixed layer (deeper layer below 80 m). Finally, we observe the efficiency of our new overturn validation criterion, $R_o = 0.25$ (see Fig. 4c), which yields a much closer agreement with different estimates at the above-mentioned four suspicious false overturns, while the $R_o = 0.2$ criterion (see Fig. 4b) still yields there abnormal overestima-

tion in the Thorpe scale-derived diffusivities (as compared to microstructure diffusivities). This confirms our previous conviction that the four suspected overturns represent really false overturns, however, these overturns escape from detection with $R_o = 0.2$ but not with $R_o = 0.25$. We have verified similar features in several other stations too, and we will use hereafter uniquely the latter criterion for the detection of false overturns.

In order to statistically evaluate the sensitivity of the vertical diffusivity to its parameterization, we have calculated for all intercomparison stations and depths the ratio of the Thorpe scale-derived diffusivities and the TurboMAP-derived diffusivities, separately using the Osborn parameterization (K_{O_T}/K_{O_E}) and the Shih parameterization (K_{S_T}/K_{S_E}) (Fig. 5). There is a clear tendency of overestimation by the Osborn parameterization especially in the layer deeper than 100 m by up to two orders of magnitude or more (Fig. 5a). Such is much less evident with the Shih parameterization which shows a comparatively much compact variability of ratio within one order of magnitude around the unity (Fig. 5b). On the other hand, in the surface layer above 100 m there is an increasing negative tendency toward the surface for both parameterizations, as already mentioned. This is probably due to a very low stratification of the surface mixed layer, which prevents to detect moderate overturns whose density differences are smaller than our threshold noise level of $7 \times 10^{-4}\,\mathrm{kg\,m^{-3}}$.

Assuming a log-normal distribution of diffusivity ratios R_{dif}, the mean and standard deviation (std) of log (R_{dif}) have been used for representing the basic statistics of R_{dif}. With the Osborn parameterization (Fig. 5c), the Thorpe scale-derived diffusivities below 200 m overestimate (compared to the TurboMAP-derived diffusivities) by a mean R_{dif} of ~ 4, with a (± 1 std) variability range of (0.7, 20), on average. The overestimation gradually diminishes toward the surface and changes its sign near 80 m to show a near surface peak of underestimation, with a mean R_{dif} of ~ 0.2 (0.01, 5). In contrast to this, the Shih parameterization (Fig. 5d) yields a much reasonable agreement, with a mean R_{dif} close to the unity (0.3, 3) over most of the water column, except for the surface layer showing always a general but somewhat reduced tendency of underestimation by ~ 0.4 (0.1, 2). Consequently, we conclude that the use of the Shih parameterization,

rather than the Osborn parameterization, is highly desirable in the estimation of vertical diffusivities.

4   Thorpe scale-derived vertical diffusivities in the KEOPS 2 area

For all KEOPS2 density profiles, we have estimated the Thorpe scale-derived vertical diffusivities K by applying the overturn criterion $R_o = 0.25$ and the Shih parameterization. Figure 6a and b represent the spatial distribution of K in the top 400 m along the approximately north–south (N–S) and east–west (E–W) oriented transects, respectively (see Fig. 1 for the position of stations). The 50 m depth-averaged K values are given in Table 1. Care is warranted to cite the values for the top 50 m depth range because of the above-mentioned underestimation tendency; a multiplication by 2 to 3 is rather recommended. The K distribution is highly heterogeneous in both the vertical and horizontal directions, varying from a low level of $< 2 \times 10^{-5} \, \text{m}^2 \, \text{s}^{-1}$ (areas with no color shading) to a relatively high level of $> 10^{-4} \, \text{m}^2 \, \text{s}^{-1}$ (areas encircled by white lines). The spatial K distribution appears to have some correlation with the regional frontal circulation carrying different water masses. For example, in the N–S transect (Fig. 6a) the areas of elevated diffusivities are mostly confined in the seasonal thermocline (< 150 m) above the Winter Water core developed to the south of the Polar Front, with the exception over the continental slope east of the Kerguelen Islands (Sts. TNS 7–9) where the diffusion rate is low. The strongest diffusivities are found over the shallow plateau (~ 600 m) southeast of the islands (Sts. TNS 10 and A3-1) and close to the PF over the northern escarpment northeast of the islands (Sts. 3–5). The diffusivity estimates at A3-1 are similar in vertical structure but smaller in magnitude by a factor of 3–4 than those estimated at the same station during the 2005 KEOPS1 cruise using the Osborn parameterization and a different method of overturn validation (Park et al., 2008). Note that most of these stations of elevated diffusivities are associated with a local patch of high chlorophyll or its downstream extension, with the exception at TNS 5 where a local minimum in chlorophyll is observed instead (see Fig. 1b). On the

Full Screen / Esc

Printer-friendly Version

Interactive Discussion

other hand, the Winter Water layer (150–250 m) generally coincides with the layer of diffusivity minimum. In Subantarctic waters north of the Polar Front (Sts. TNS 1–2), on the contrary, the diffusion rate is quite low throughout the upper 400 m, resting close to its background level of $O(10^{-5}\,m^2\,s^{-1})$.

On the E–W transect (Fig. 6b), the spatial distribution of K is quite complex compared to the N–S section and there does not appear any simple pattern that can be easily connected to the frontal circulation of water masses. Nevertheless, we remark a relatively strong diffusion rate of $O(10^{-4}\,m^2\,s^{-1})$ over much of the water column at E1–4W that is located close to the northward flowing PF along the escarpment east of the Kerguelen Islands, while the weakest rate of $O(10^{-5}\,m^2\,s^{-1})$ is observed at TEW7 where an apparent southward intrusion of relatively warm Subantarctic surface water is associated with the southward retroflecting PF (see Fig. 1b). Other stations on the section show a highly undulating vertical structure with a moderate diffusion rate of $< 5 \times 10^{-5}\,m^2\,s^{-1}$, in general.

5 Concluding remarks

We have validated the Thorpe scale-derived vertical diffusivities in the PF region east of the Kerguelen Islands in comparison with more direct estimates from the TurboMAP microprofiler measurements at selected stations during the KEOPS2 cruise. We have emphasized the need of a careful treatment of raw CTD data to obtain density profiles as fine as possible but with a maximum removal of random noise and measurement errors. The comparative results are found to be sensitive to the choice of the parameterization of diffusivity and the overturn validation criteria. The use of the Shih parameterization (Eqs. 2 and 5) combined with a new overturn criterion of $R_o = 0.25$ has yielded far better results by a factor of 5 compared to the results obtained from the Osborn parameterization (Eqs. 1 and 6) and the $R_o = 0.2$ criterion (Gargett and Garner, 2008). The latter criterion is found to be insufficient in our case to detect and remove false overturns that cause an abnormal overestimation in the Thorpe scale-derived dif-

fusivities. The Osborn parameterization is found to be much more sensitive to such an overestimation compared to the Shih parameterization. This study demonstrates that the Thorpe scale method is still a useful tool for studying the fine scale diffusivities in the upper layer of the ocean if one makes judicious use of the combined Shih parameterization and $R_o = 0.25$ criterion.

The Thorpe scale-derived vertical diffusivities in the KEOPS2 region vary from a background level of $O(10^{-5}\,\mathrm{m}^2\,\mathrm{s}^{-1})$ in the Winter Water layer to a relatively high level of $O(10^{-4}\,\mathrm{m}^2\,\mathrm{s}^{-1})$ in the seasonal thermocline above the Winter Water. The latter feature is especially pronounced at stations over the shallow plateau southeast of the Kerguelen Islands and in the cold side of the PF running along the escarpment northeast of the islands. On the other hand, at stations immediately north of the PF where warmer Subantarctic surface waters are encountered, diffusivity values are particularly low.

References

Dillon, T. M.: Vertical overturns: a comparison of Thorpe and Ozmidov length scales, J. Geophys. Res., 87, 9601–9613, 1982.

Ferron, B., Mercier, H., Speer, K., Gargett, A., and Polzin, K.: Mixing in the Romanche fracture zone, J. Phys. Oceanogr., 28, 1929–1945, 1998.

Frants, M., Damerell, G. M., Gille, S. T., Heywood, K. J., MacKinnon, J., and Springtall, J.: An assessment of density-based finescale methods for estimating dyapycnal diffusivity in the Southern Ocean, J. Atmos. Ocean. Tech., 30, 2647–2661, 2013.

Galbraith, P. S. and Kelley, D. E.: Identifying overturns in CTD profiles, J. Atmos. Ocean. Tech., 13, 688–702, 1996.

Gargett, A. and Garner, T.: Determining Thorpe scales from ship-lowered CTD density profiles, J. Atmos. Ocean. Tech., 25, 1657–1670, 2008.

Klymak, J. M., Pinkel, R., and Rainville, L.: Direct breaking of the internal tides near topography: Kara Ridge, Hawaii, J. Phys. Oceanogr., 38, 380–399, 2008.

Osborn, T. R.: Estimates of the local rate of vertical diffusion from dissipation measurements, J. Phys. Oceanogr., 10, 83–89, 1980.

Ozmidov, R. V.: On the turbulent exchange in a stably stratified ocean, Izv. Atmos. Ocean. Phy., 1, 853–860, 1965.

Park, Y.-H., Fuda, J. L., Durand, I., and Naveira Garabato, A. C.: Internal tides and vertical mixing over the Kerguelen Plateau, Deep-Sea Res. Pt. II, 55, 582–593, 2008.

Park, Y.-H., Durand, I., Kestenare, E., Rougier, G., Zhou, M., d'Ovidio, F., Cotté, C., and Lee, J.-H.: Polar front around the Kerguelen Islands: an up-to-date determination and associated circulation of surface/subsurface waters, J. Geophys. Res., submitted, 2014.

Shih, L. H., Koseff, J. R., Ivey, G. N., and Ferziger, J. H.: Parameterization of turbulent fluxes and scales using homogeneous sheared stably stratified turbulence simulations, J. Fluid Mech., 525, 193–214, 2005.

Thorpe, S. A.: Turbulence and mixing in a Scottish loch, Philos. T. Roy. Soc. Lond., 286A, 125–181, 1977.

Validation of the Thorpe scale-derived vertical diffusivities

Y.-H. Park et al.

Full Screen / Esc

Printer-friendly Version

Interactive Discussion

Table 1. 50 m averaged vertical diffusivities (in $10^{-5}\,\mathrm{m^2\,s^{-1}}$) at A3-1 estimated from the Thorpe scale method using the Shih parameterization and the $R_o = 0.2$ criterion.

| Station	depth range (m)							
	0–50	50–100	100–150	150–200	200–250	250–300	300–350	350–400
TNS10	44	37	34	2	6	1	5	2
TNS09	22	5	1	4	2	1	6	19
TNS08	18	8	1	8	1	3	6	7
TNS07	2	2	1	1	2	2	12	5
TNS06	34	11	7	4	2	6	3	2
TNS05	16	18	13	1	9	9	5	2
TNS04	67	19	5	1	1	11	1	2
TNS03	16	22	27	2	2	3	6	1
TNS02	1	1	1	1	1	5	1	1
TNS01	1	4	3	1	1	3	1	1
TEW01	20	4	NaN	NaN	NaN	NaN	NaN	NaN
TEW02	1	1	NaN	NaN	NaN	NaN	NaN	NaN
TEW03	1	4	2	3	1	21	2	1
TEW04	1	2	5	4	2	2	7	2
TEW05	1	6	1	3	2	8	4	4
TEW06	1	2	7	1	2	4	1	5
TEW07	1	1	7	1	1	2	3	2
TEW08	2	4	1	2	2	11	7	9
A3-1	13	18	13	2	1	1	2	5
E1-2	4	1	3	6	1	2	6	2
E1-4W	9	19	24	14	19	7	1	9
NPF-L	6	5	6	18	2	3	6	3

Full Screen / Esc

Printer-friendly Version

Interactive Discussion
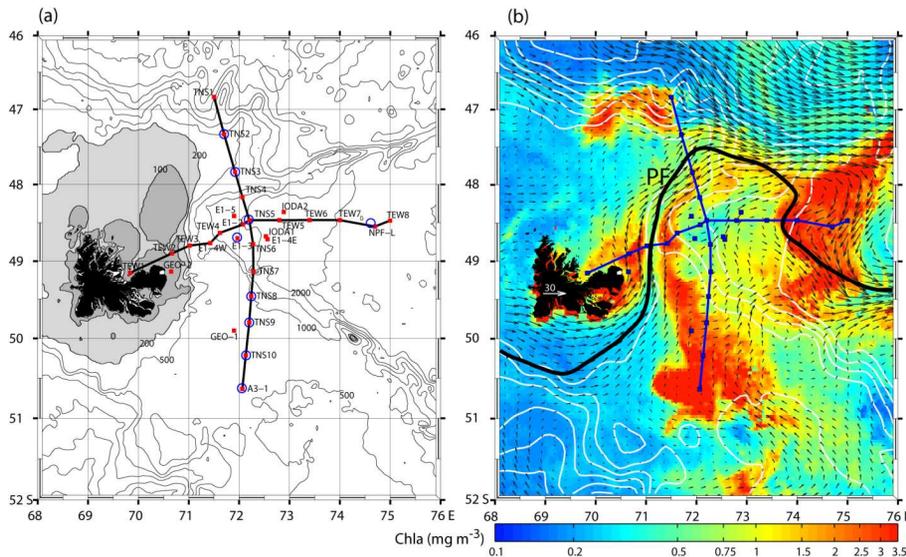
Figure 1. (a) Map showing the KEOPS2 CTD stations (red dots) on or close to two N–S and E–W transects superimposed on the detailed bathymetry. The concomitant TurboMAP microprofiler stations are indicated by blue circles. Isobaths greater than 500 m are given every 500 m and the seabed shallower than 200 m (100 m) is lightly (darkly) shaded. (b) These stations are also superimposed on a representative satellite image of chlorophyll concentration (colors) and a surface geostrophic velocity field (arrows) constructed from the combined data sets from altimetry and trajectories of drifters launched during the cruise. The geographical position of the Polar Front (PF) is indicated. Adapted from Park et al. (2014).
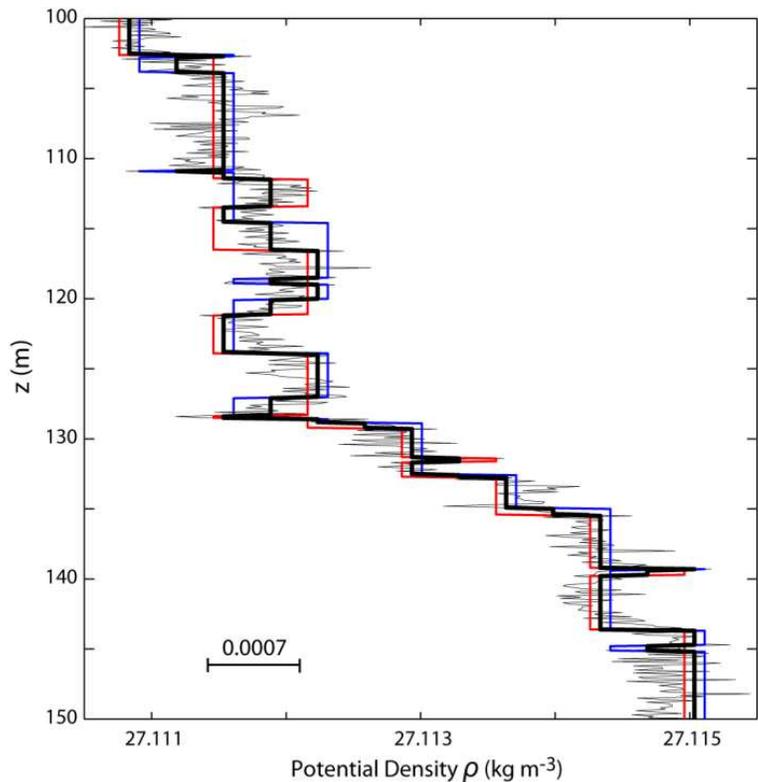
Figure 2. Sample section of intermediate profiles generated from the top (red), from the bottom (blue), and from the average of these two (thick black) of a measured density profile (thin black), following the method of Gargett and Garner (2008). The threshold density noise used is indicated.

Title Page

Abstract | Introduction

Conclusions | References

Tables | Figures

|◄ | ►|

◄ | ►

Back | Close

Full Screen / Esc

Printer-friendly Version

Interactive Discussion
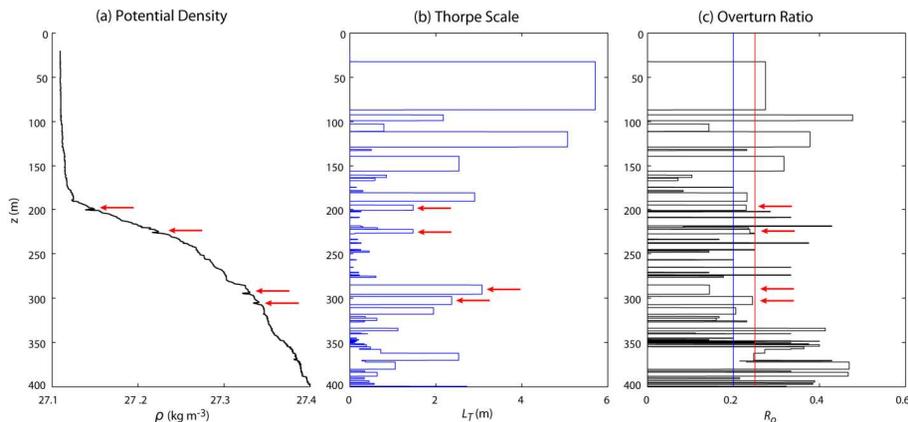
Figure 3. Sample illustration showing the **(a)** intermediate density profile, **(b)** Thorpe scales, and **(c)** overturn ratios calculated at A3-1. Four suspicious false overturns most apparent in the density profile are indicated by red arrows. Two criteria of overturn validation are shown by coloured vertical lines in **(c)**: blue for $R_o = 0.2$ and red for $R_o = 0.25$.
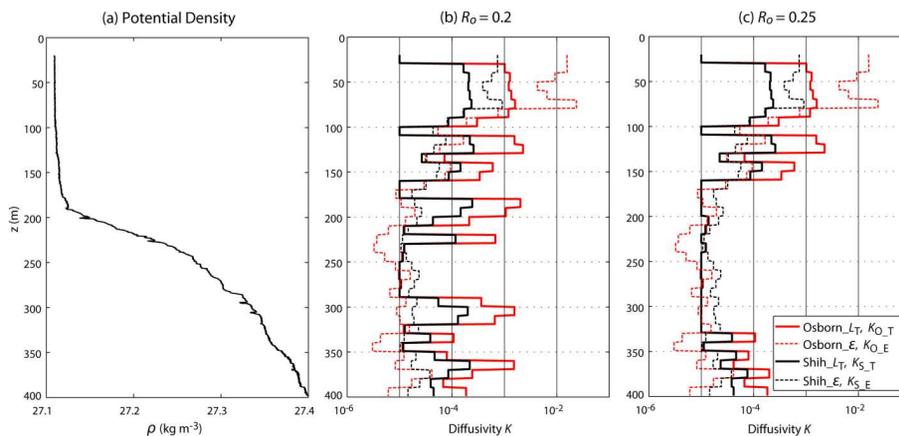
Figure 4. Different diffusivity profiles at A3-1 calculated with different pairs of parameterization (Osborn or Shih) and observational method (Thorpe scale L_T or TurboMAP-derived ε) using the two overturn validation criteria of **(b)** $R_o = 0.2$ and **(c)** $R_o = 0.25$. Note that the four suspicious overturns seen in **(a)**, which being the repetition of Fig. 3a, give rise to abnormal overestimation in the Thorpe scale-derived diffusivities with $R_o = 0.2$, but such a feature disappears completely with $R_o = 0.25$.
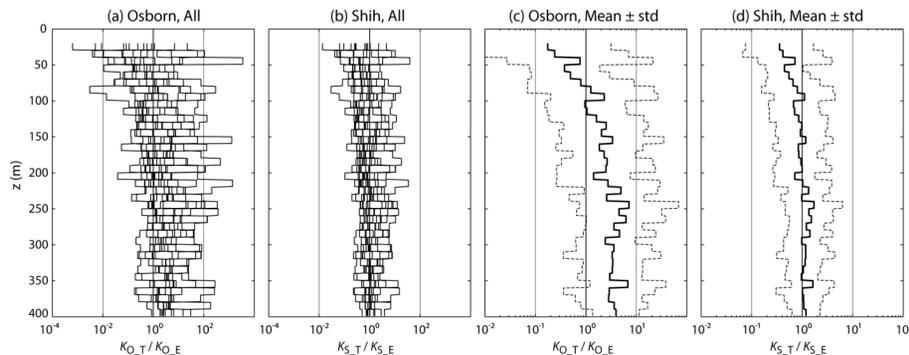
Figure 5. Ratio profiles of the Thorpe scale-derived diffusivities and the TurboMAP-derived diffusivities at all intercomparison stations based on **(a)** the Osborn parameterization and **(b)** the Shih parameterization. Here, the $R_o = 0.25$ criterion is commonly used. **(c)** and **(d)** are same as **(a)** and **(b)** but for mean (± std) ratios of all stations.
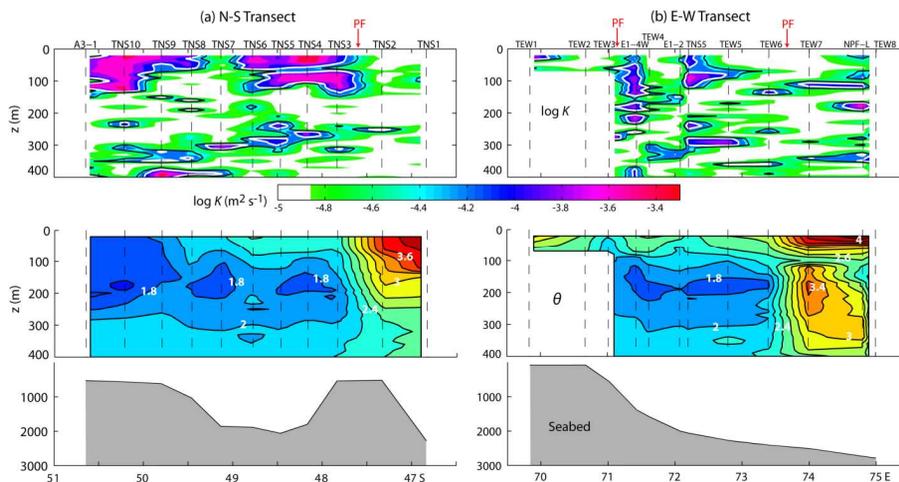
Figure 6. Thorpe scale-derived diffusivity sections (calculated using the Shih parameterization and the $R_o = 0.25$ criterion) of the upper 400 m on **(a)** the N–S transect and **(b)** the E–W transect (top panels; see Fig. 1 for locations of the transects and stations). Diffusivity K values, which range from $10^{-5}\,\mathrm{m^2\,s^{-1}}$ to $7 \times 10^{-4}\,\mathrm{m^2\,s^{-1}}$, are shown in log (K). White and black lines correspond to $K = 10^{-4}\,\mathrm{m^2\,s^{-1}}$ and $K = 5 \times 10^{-5}\,\mathrm{m^2\,s^{-1}}$, respectively, while the regions without colour shading to $K < 2 \times 10^{-5}\,\mathrm{m^2\,s^{-1}}$. For easy of interpretation in combination with the 3-D frontal circulation of water masses (see also Fig. 1), corresponding temperature sections (middle panels) and seabed profiles (bottom panels) are also shown.